Supporting Information

Stabilizing Sulfur Vacancy Defect by A "Click" Chemistry of Ultrafine Palladium to Trigger High-Efficiency Hydrogen Evolution of MoS$_2$

Suli Liu,[* a] liangliang Zhou,[a] Wanjia Zhang,[a] Junyu Jin,[a] Xueqin Mu,[a] Sudi Zhang,[a] Changyun Chen,[a] and Shichun Mu[*b]

[a]Department of Chemistry, Nanjing Xiaozhuang University, Nanjing, Jiangsu 211171, P. R. China.

[b]State Key Laboratory of Advanced Technology for Materials Synthesis and Processing, Wuhan University of Technology, Wuhan, Hubei 430056, P. R. China.

E-mail: niuniu_410@126.com; msc@whut.edu.cn.

1. Electrochemical HER measurements

The electrochemical HER experiment was carried out on a CHI 660E electrochemical workstation (Shanghai, Chenhua Co.) with a standard three electrode system. A graphite rod electrode served as the counter electrode, while Ag/AgCl (3 M KCl) acted as the reference electrode and a glassy carbon electrode (GCE) (3 mm in diameter) was used as the working electrode. The catalyst dispersions were prepared by mixing a certain amount of catalyst with the appropriate amount of water, ethanol, and Nafion (1.0 wt%) with a volume ratio of 3.8:1:0.2 under sonication for 40 min to form a homogeneous ink with a concentration of 5 mg mL^{-1}. The catalyst suspension (4 µL) was dropped onto the GCE surface and air dried. All the modified electrodes were pretreated by cycling the potential between -0.80 and 0.10 V for 100 cycles to remove any surface contamination prior to the electrochemical test. Cyclic voltammetry (CV) measurements were conducted in N$_2$-saturated 0.5 M H$_2$SO$_4$, 1.0 M PBS, and 1.0 M KOH aqueous solutions. All the potentials were referenced to a reversible hydrogen electrode (RHE).

2. Method and Model

The surfaces of 1T(001) and 1T(100) have been built with and without the Co doped, then the Pd cluster has been loaded on the Co doped systems, where the vacuum space along the z direction is set to be 15 Å, which is enough to avoid interaction between the two neighboring images. All atoms are relaxed. Then, the H atoms have been absorbed on the surface of substrate, respectively, where the two different absorption sites of Pd and Co atoms have been considered. The first principles calculations in the framework of density functional theory were carried out based on the Cambridge Sequential Total Energy Package known as CASTEP.[1] The exchange–correlation functional under the generalized gradient approximation (GGA)[2] with norm-conserving pseudopotentials and Perdew–Burke–Ernzerhof functional was adopted to describe the electron–electron interaction.[3] An energy cutoff of 750 eV was used and a k-point sampling set of 5 x 5 x 1 were tested to be converged. A force tolerance of 0.01 eV Å^{-1}, energy tolerance of 5.0 x 10^{-7} eV per atom and maximum displace-ment of 5.0 x 10^{-4} Å were considered.

Thermodynamics and photocatalysis

Adsorption energy ΔE of H atom on the surface of substrates was defined as:

$$\Delta E = E_{*H} - (E_* + E_H) \tag{2}$$

where *H and * denote the adsorption of H atom on substrates and the bare substrates, E_H

denotes the half of energy of H_2.

Free energy change ΔG of the reaction was calculated as the difference between the free energies of the initial and final states as shown below:

$$\Delta G = \Delta E + \Delta ZPE - T\Delta S \tag{3}$$

where E is the calculated energy by DFT, ZPE is the zero point energy, S denotes the entropy, The value of ($\Delta ZPE - T\Delta S$) is 0.24 eV,[4] $\Delta G = \Delta E + 0.24$eV.

[1] M. D. Segall, P. J. D. L. M. J. Probert, C. J. Pickard, P. J. Hasnip, S. J. Clark and M. C. Payne, *J. Phys.: Condens. Matter* **2002**, *14*, 2717.

[2] J. P. Perdew, K. Burke and M. Ernzerhof, *Phys. Rev. Lett*. **1996**, *77*, 3865.

[3] D. R. Hamann, M. Schl¨ uter and C. Chiang, *Phys. Rev. Lett.* **1979**, *43*, 1494.

[4] D. Voiry,H. Yamaguchi,J. Li, R. Silva, D. C. B. Alves,T. Fujita, M. W. Chen,T. Asefa,V. Shenoy, G. Eda, M. Chhowalla, *Nat. Mater.* **2013**, *12*, 850-855.

Table S1. DFT calculation analysis of different catalysts.

Catalyst	ΔG_H
1T MoS_2 (100)	-1.11
1T $Co\text{-}MoS_2$ (100)	-0.35
1T Pd modulated $Co\text{-}MoS_2$ (100)	-0.23
1T MoS_2 (001)	0.74
1T $Co\text{-}MoS_2$ (001)	-0.52
1T Pd modulated $Co\text{-}MoS_2$ (001)	-0.40
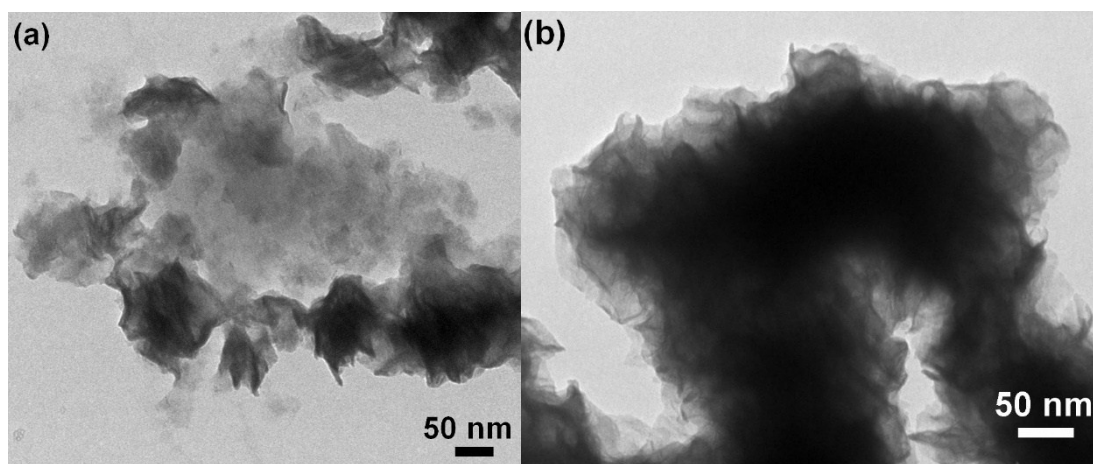
Figure S1. Low-magnification TEM images of (a) MoS_2 NSs and (b) $Co\text{-}MoS_2$ NSs.
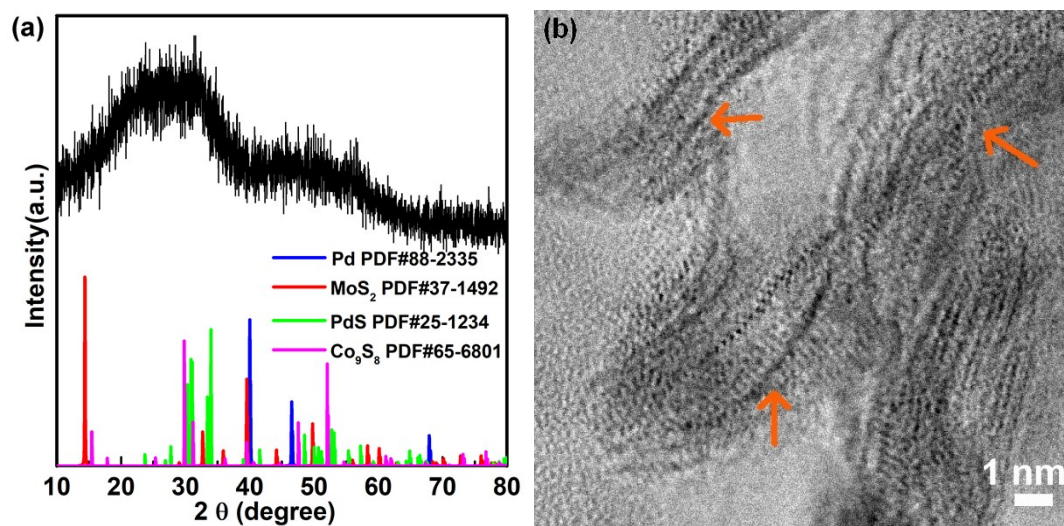
Figure S2. (a) XRD patterns and (b) HRTEM image of Pd modulated $Co\text{-}MoS_2$ NSs.
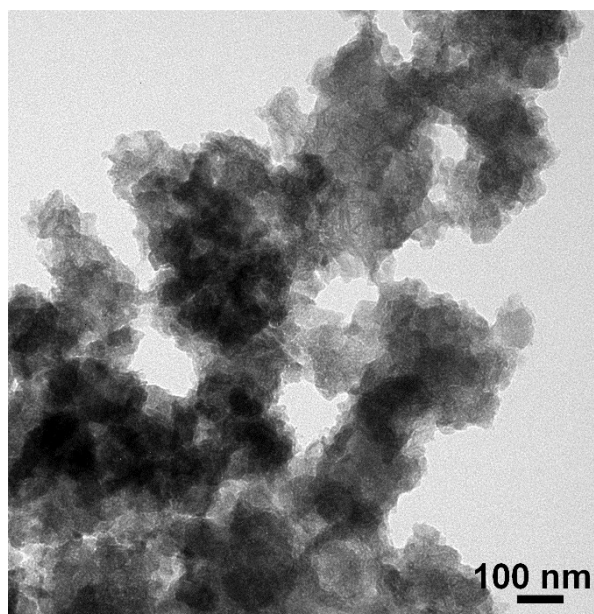
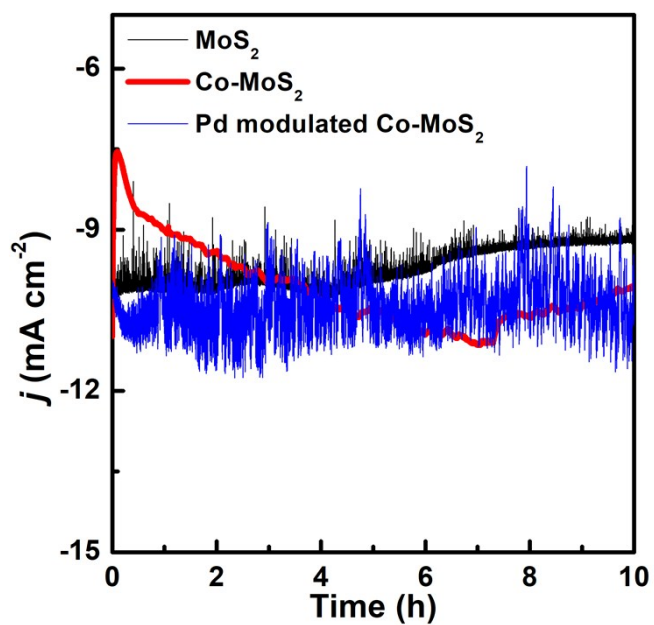**Figure S3**. TEM image of as-synthesized Pd modulated Co-MoS$_2$ NSs after the HER properties in 0.5 M H$_2$SO$_4$.

Figure S4. Stability measurement for MoS$_2$, Co-MoS$_2$ NSs and at Pd modulated Co-MoS$_2$ NSs η_{10} in 0.5 M H$_2$SO$_4$.
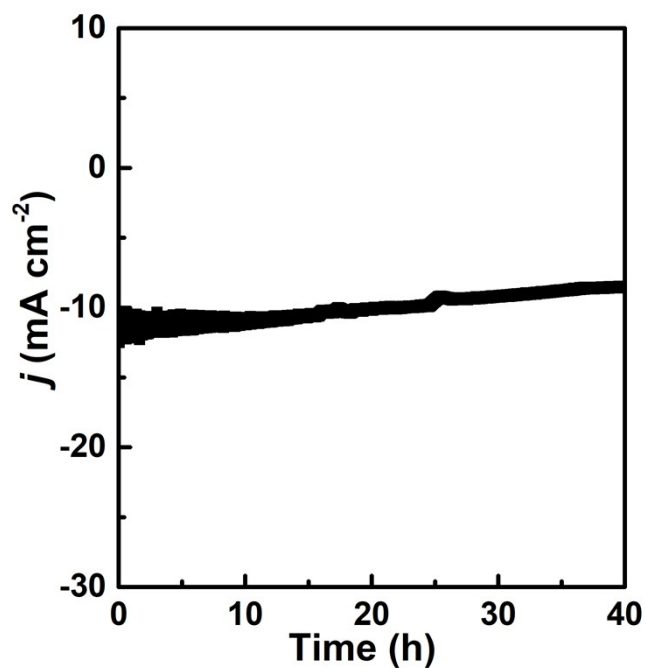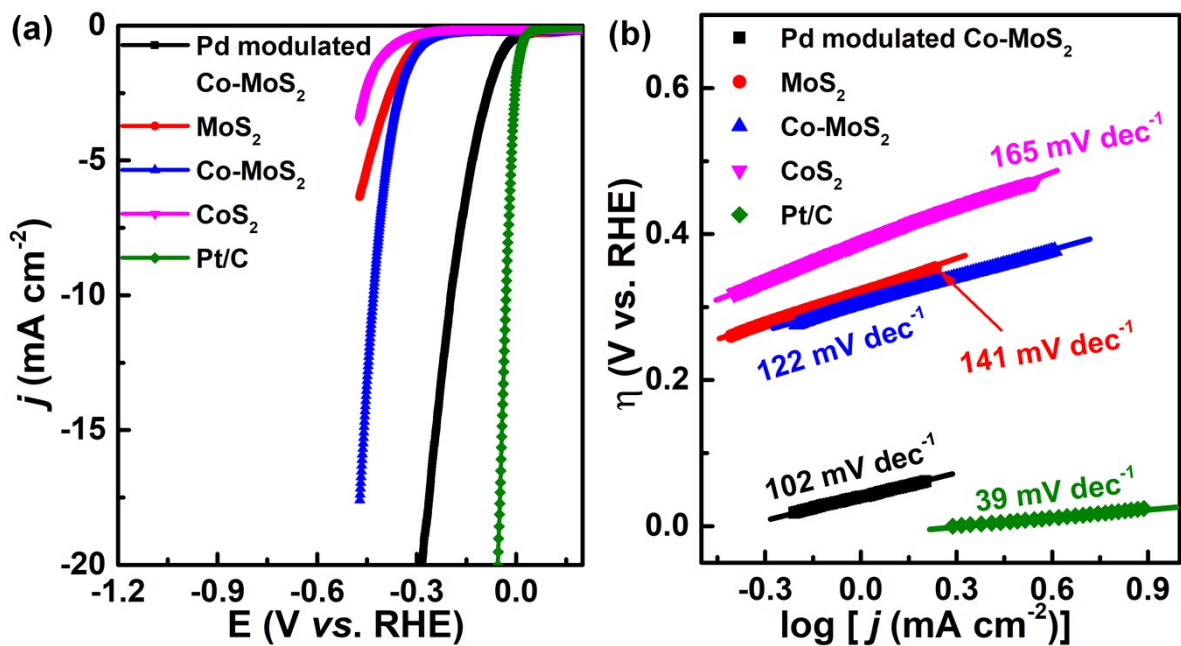
Figure S5. Stability measurement for Pd modulated Co-MoS$_2$ NSs at η_{10} in 1.0 M PBS.
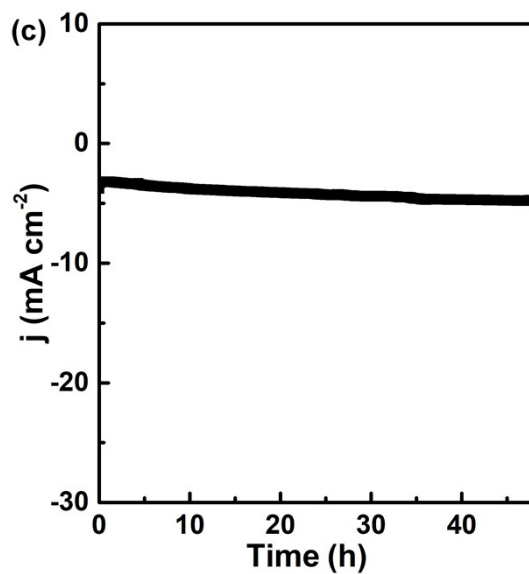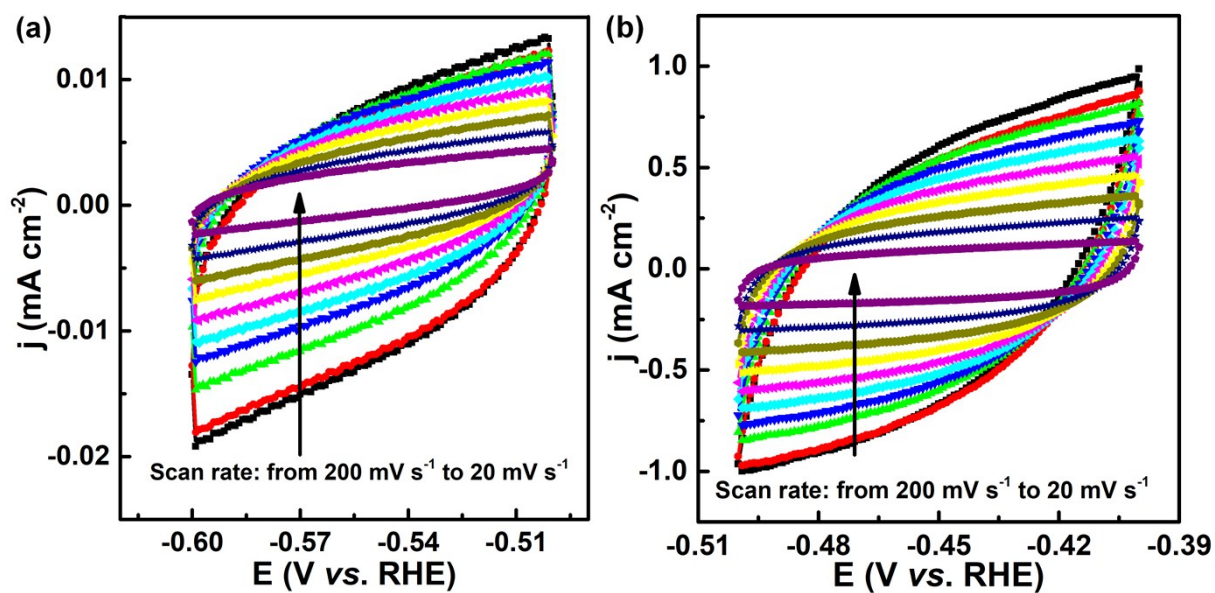
Figure S6. (a) Polarization curves of CoS_2, MoS_2, $Co\text{-}MoS_2$, Pd modulated $Co\text{-}MoS_2$ NSs, and Pt/C in 1.0 M KOH. (b) Corresponding Tafel plots. (c) Stability measurements for Pd modulated $Co\text{-}MoS_2$ NSs in 1.0 M KOH.
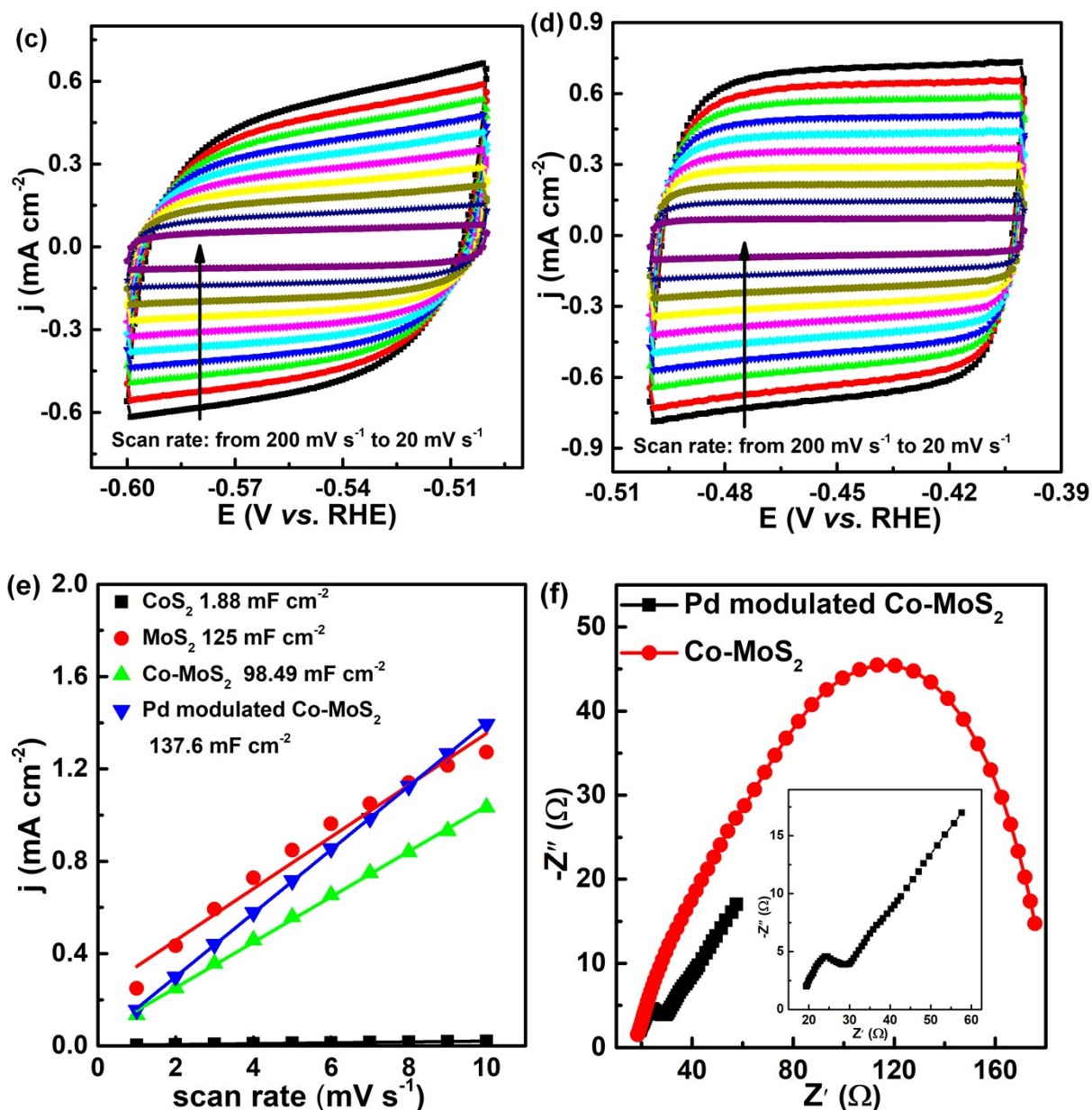
Figure S7. Cyclic voltammograms measured in a non-Faradaic region for (a) CoS_2, (b) MoS_2, (c) Co-MoS$_2$, and (d) Pd modulated Co-MoS$_2$ NSs at various scanning rates. (e) Estimation of double layer capacitances for CoS_2, MoS_2, Co-MoS$_2$, and Pd modulated Co-MoS$_2$ NSs using the capacitive current densities at 0.1 V (vs RHE) as a function of scan rates. (f) Nyquist plots of the as-prepared samples in modified electrodes recorded at a constant overpotential of 250 mV.

Table S2. Comparison of HER activities of metal sulfides catalysts in 0.5 M H_2SO_4.

Materials	η_{10} (mV)	Tafel slope (mV dec^{-1})	Stability (h)	Ref.
Pd modulated Co-	92	42	40	This work

MoS$_2$ NSs				
amorphous CoMoS	200	198	/	*ACS Catal.* **2012**, *2*, 1916-1923.
CoMoS$_3$	143	78	10	*J. Mater. Chem. A* **2017**, *5*, 11309-11315.
Ni–Co–MoS$_2$	125	51	12	*Adv.Mater.* **2016**, *28*, 9006-9011.
MoO$_3$@MoS$_2$	235	50	/	*Nano Lett.* **2011**, *11*, 4168-4175.
CoMoS$_4$/CC	80	105	/	*Nanosacle* **2016**, *8*, 18887-18892.
superaerophobic MoS$_2$	200	51	5.8	*Adv. Mater.* **2014**, *26*, 2683-2687
metallic MoS$_2$	195	43	9	*J. Am. Chem. Soc.* **2013**, *135*, 10274-10277.
MoS$_2$/CNT-graphene	255	100	/	*ACS Nano* **2014**, *8*, 5164-5173.
Co-doped MoS$_2$ with CoMoS phase	~220	~87	5000 cycles	*ACS Appl. Mater. Interfaces* **2015**, *7*, 27242-27253.
CoMoS/CoMoO$_4$/ /NRGO	80	58	1000 cycles	*J. Mater. Chem. A* **2017**, *5*, 2885-2896

Table S3. Comparison of HER activities of metal sulfides catalysts in 1.0 M PBS.

Materials	η10 (mV)	Tafel slope (mV dec-1)	Stability (h)	Ref.
Pd modulated Co-MoS$_2$ NSs	60	56	40	This work
CoP/CC	65	51	22	*J. Am. Chem. Soc.* **2014**, *136*, 7587–7590.
Co$_9$S$_8$/CC	175	/	10	*J. Mater. Chem. A* **2016**, *4*, 6860-6867.
CuMoS$_4$ crystals	135	95	/	*Energy Environ. Sci.* **2012**, *5*, 8912-8916.

CoO/CoSe$_2$	337	131	10	*Adv. Sci.* **2016**, *3*, 1500426.
Co@S/FTO	287	93	40	*J. Am. Chem. Soc.* **2013**, *135*, 17699-17702.
Co@B pellets	251	/	1000 cycles	*J. Power Sources* **2015**, *279*, 620-625.
Co-Mo-S film/GC	200	87	/	*Chem. Sci.* **2012**, *3*, 2515-2525.
MoS$_2$/N-doped graphene	261	117	/	*J. Mater. Chem. A* **2014**, *2*, 13795.
Ni$_3$S$_2$/NF	170	/	200	*J. Am. Chem. Soc.* **2015**, *137*, 14023-14026.